

Виконано тривимірне чисельне розв'язання тестової задачі про течію в'язкої нестисливої рідини в закритій квадратній каверні з рухомою верхньою гранню. Вказано недоліки математичної постановки задачі про течію рідини в закритій каверні. Методом скінчених елементів проведено чисельне дослідження структури циркуляційного відривного ламінарного руху в'язкої нестисливої рідини у відкритій каверні з урахуванням зовнішньої течії. Наведено профілі завихорості, товщини пограничного шару, складових компонент швидкості у різних перерізах каверні, в пограничному шарі, а також у шарі змішування.

Зазвичай при дослідженні ламінарних течій в кавернах використовують модель каверні з рухомою стінкою. Але використання задачі за такої постановки накладає обмеження на картину течії у вигляді прямолінійної лінії течії, яка з'єднує верхні кути каверні, що призводить до невірної структури вихороутворення в каверні у цілому. В рамках даного дослідження запропоновано постановку задачі, яка долає вказаний недолік. Рух рідини в каверні здійснюється за рахунок напруження зсуву зовнішнього потоку в каналі над каверною, що виключає прямолінійність лінії течії, яка з'єднує кутові точки каверні. Достовірність отриманих результатів підтверджена порівнянням деяких параметрів з відомими експериментальними даними інших авторів. Отриманий науковий результат у вигляді структури вихороутворення в'язкого нестисливого ламінарного потоку у відкритій каверні з каналом є цікавим з теоретичної точки зору. З практичної точки зору виявлена структура течії дозволяє визначити умови керування потоком в каверні, і, отже, дозволяє визначити умови оптимізації аеродинамічних сил, діючих на каверну. Прикладним аспектом використання отриманого наукового результату є можливість застосування його до обткання об'єктів промисловості: будівель, міжвагонного простору залізничного потяга та ін.

Ключові слова: відрив потоку, ламінарний режим, течія в каверні, чисельне моделювання, структура вихороутворення

UDC 532.517: 536.24
DOI: 10.15587/1729-4061.2019.183811

DETERMINING THE STRUCTURE OF A LAMINAR DETACHABLE CURRENT IN AN OPEN CAVITY

E. Kravets

PhD, Associate Professor
Department of AeroHydro Mechanics and Energy and Mass Transfer
Oles Honchar Dnipro National University
Gagarina ave., 72,
Dnipro, Ukraine, 49010
E-mail: kravets974@ukr.net

Received date 29.08.2019

Accepted date 15.11.2019

Published date 23.12.2019

Copyright © 2019, E. Kravets

This is an open access article under the CC BY license
(<http://creativecommons.org/licenses/by/4.0>)

1. Introduction

Flow detachment is the phenomenon of separating part of a current from the solid wall of a streamlined body, caused by the simultaneous action of many factors. Specifically, as indicated in [1, 2], the classic concept of flow detachment is related to the viscosity property of a liquid or a gas. The presence of viscosity forces when a medium flows over a solid wall gives rise to the emergence of tangent forces that counteract movement and cause the flow to brake near the wall. Reducing the medium movement speed near the wall forms a boundary layer – a layer of inhibited environment in close proximity to the streamlined rigid surface.

Therefore, the flow detachment is often referred to as a detachment of the boundary layer [1]. A positive pressure gradient in the direction of the current is also a necessary condition for a viscous current detachment [1]. In the absence of one of these two conditions, the flow detachment does not occur. The author of book [3] confirms that the danger of a border layer detachment always exists in the regions with increasing pressure, citing an example of the detachable flow over bodies with a blunt stern. He also notes the mechanism of the flow detachment occurrence: “due to the formation of a reciprocal current near the wall there is a strong thickening of the boundary layer, which entails the removal of liquid from the boundary layer into the outer current.” The detachment point location can be determined theoretically, based on the zero speed gradient level limit in the direction perpendicular to the wall [3]:

$$\left(\frac{\partial U}{\partial y}\right)_{wall} = 0. \quad (1)$$

Flow detachment can turn out to be both the useful and negative phenomenon, making it difficult for devices and structures to work. Thus, paper [1] notes that a flow detachment leads to additional energy scattering. At the same time, it is specified that in the current's subsonic region the resistance of the streamlined body grows, the lift force decreases, the stagnant zone and return flow zone are formed. There is also a negative effect exerted by flow detachment on the internal currents in various hydraulic machines (turbines, pumps, compressors), which is revealed by a decreased efficiency.

However, the flow detachment might prove, in some situations, to be a phenomenon that could improve characteristics of a streamlined body. Paper [1] gives an example when a thin body, designed for high-speed flights, is flown over at low speeds: the profile is artificially thickened by creating a flow detachment on the section of its upper surface, followed by the flow attachment.

2. Literature review and problem statement

A stable flow detachment and the circulating fluid current formation are often studied based on the problem about fluid movement in a cavity with a moving wall. In this case, the current mechanism is described by the following classic

pattern: when a lid moves, the layer of liquid directly adjacent to it becomes movable, the movable layer then involves ever deeper layers of liquid up to the bottom of a cavity. Such a statement automatically assumes the directness of a current line (a plane for a three-dimensional case), connecting the upper corners of the cavity and coinciding, in this case, with the movable lid. In fact, when the rectangular or square cavities are flown around, a given current line is not rectilinear but, according to study [4], is convex towards the channel over the cavity.

This disadvantage is eliminated in the statement of a problem about a current in the open cavity, taking into consideration the external flow, whose scheme is given in [1]. As also indicated in [1], due to the pulsations of the separating line of current in the interval $\pm\Delta$ near the middle position the cavity receives a mass of liquid that circulates around the vortex of compression, it enters a free viscous layer and flows beyond the compression point.

An overview of studies into the hydrodynamics of detachable currents in cavities up to 2009 could be found in the [6–8]. The pattern of vortex formation and the mechanism of heat exchange when a medium moves in a spherical cavity are described in [9] where the status of this issue and the problems related to solving the problem are detailed. The authors considered issues regarding the structure of a circulation movement when spherical excavations are flown around, and described features of the mechanism that forms a tornado-like vortex at flow detachment. That review was a generalization of studies reported in earlier papers by the author, for example [10], which described results of an experiment to investigate the local heat output from a single deepening in the spherical shape on the wall of a rectangular channel. The results obtained were also compared to available data on the intensity of heat and mass exchange for semi-spherical cavities and cylindrical recesses at the surface. In this case, there were the unresolved issues related to determining pressure pulsations in the flow over a cavity and examining the process of current's transition to the resonance state. These issues were addressed in work [12], whose authors conducted an experimental study of the flow around an isolated small open-type cavity. Pressure pulsations were measured at the Mach numbers for an unperturbed flow of 0.3, 0.5, and 0.6 for two cavity models. The pulsation characteristics of pressure were investigated by the Fourier transforms, wavelets, and Gilbert transformations. However, the authors did not address the impact of the geometry of a cavity's edge on the current down the flow.

Results from study [12] suggested that the structure of a detachable current is affected not only by the current speed, the shape and geometric size of the hole that simulates the cavity, but also the geometry of its edge. The study notes that when the hole, which has a sharp edge, is flown around, there forms a massive vortex of toroidal shape, and its intensity increases with the increase in the depth of the hole. If the edge of the hole is smoothed, the vortex above it is almost not formed, and the flow flows along the surface without interruption.

Of applied character, in solving the conjugated problems of hydrodynamics and thermal exchange, is the series of papers that employ a joint solution to the equations of motion and energy [13–28]. If one examines, in the problem on a medium's motion in a cavity, the joint effect of the fields of speed, pressure, and temperature, a given problem then could be applied when the heat exchange is intensified. Study [13]

considers some promising methods to increase the intensity of convective heat exchange in pipes (ribs, pins, holes) and gives a comparison of their heat hydraulic characteristics. The authors demonstrated the effect of the specified characteristics on the parameters of a heat exchange apparatus. It is noted that despite the relatively small magnitude of heat exchange intensification, the sunken surfaces make it possible to significantly improve the efficiency of heat exchange equipment.

Of interest is a study reported in work [14] into the effect of flow control on heat exchange in a three-dimensional rectangular cavity. The authors established patterns in current lines, isotherms, and identified regions with the maximum and minimum energy dissipation values. Paper [15] analyzes the process of thermal stirring in a cavity from the heated bottom. The highest degree of stirring was found at the maximal speed of the lid movement among the examined ones, as well as when cooling the side wall. The authors of work [16] consider free convection in a square cavity, as well as near the hot horizontal cylinder.

The aim of paper [17] was to study numerically the natural convection heat exchange in a cubic cavity, caused by the thermally active plate. The influence of the plate size and its orientation relative to the vector of gravity force on the convective heat exchange and the flow structure inside a cavity has been studied and highlighted. Work [18] numerically studies a laminar mixed convection in the cavity at different configurations of heating of its walls.

All the above studies considered only Newtonian fluids as an environment. This shortcoming was overcome in work [19], which investigated the processes of natural convection of nanofluids in a vertical rectangular channel with a porous filler. Studies into the laminar natural convection of a non-Newtonian fluid in cavities were reported in papers [20, 21]. A problem of the joint forced and free laminar convection for a liquid with variable viscosity was solved in [22]. A numerical forecast of natural convection in a closed deep rectangular cavity was given in [23]. The authors of work [24] presented a numerical study of laminar heat transfer by natural convection in a closed cavity with two elliptical cylinders at different vertical distributions relative to each other.

The authors of paper [25] study effect of the geometric position of a heat source on the character and current in a cavity by calculating four different configurations of discretely heated cavities.

In contrast to other studies, work [26] investigated current and heat exchange in a cavity with sloping walls. The structure of the current was found to be affected by four dimensionless parameters, including the inclination angle of the cavity walls.

In [27], authors proposed a method of calculating the free-convective current of a viscous incompressible environment in a rectangular cavity. Side walls of the cavity have the same constant temperature, the upper and lower walls are thermally insulated, and the ratio of half-width to height is much less than unity. The decomposition of the flow region into zones with upward and downward flows made it possible to formulate and solve analytically an interrelated parabolic system of linear equations based on the classic assumptions by Oberbek-Boussinesq. The thermal modes of deep cavities were simulated in [28].

In addition to the non-Newtonian flow, article [29] performs a numerical analysis of the micropolar laminar flow of

fluid in a square cavity with a lid. The theory of micropolar fluid complements the laws of classical fluid mechanics, taking into consideration the influence of liquid's molecules on the allocated volume.

Solving a problem on studying control over flow when cavities are flown around was also addressed in work [30], whose authors examined the physics of a flow in a cavity while it was being managed. Two models were considered: a laminar flow around a square cavity at Reynolds number $Re=7,500$ and the turbulent current modes in deep cavities under a transonic mode. A very good alignment between the results and experiments was obtained.

The theory of optimal control was also applied by the author of work [31] to reduce the level of noise emitted by the cavity when it is streamlined. Typically, a mathematical model for the problem on studying the emergence and features of the development of acoustic vibrations when a cavity is streamlined employs a Navier-Stokes motion equations for the medium taking into consideration the compression effects, which leads to large computing costs. To address this issue, the cited work proposes using a reduced-order model (ROM) based on the proper orthogonal decomposition (POD), which is an adjusted approach to direct simulation of the system of differential equations.

The above suggests that it is an expedient task to investigate the hydrodynamics in the flow around open cavities given the wide scope of possible application of the results from solving this problem. Thus, study [32] examines a classic problem on the current in a cavity caused by the shear stress, with the aim of applying it in the field of two-phase cooling systems, as well as in the technologies for applying a surface coating in the form of a thin film. The cited work numerically explores the effect of cavity geometry on the three-dimensional field of velocities.

Paper [33] investigated theoretically and experimentally a three-dimensional instability of stationary laminar two-dimensional currents, which occur in a cavity with an equilateral triangular cross-section when its lid is moving.

Work [33] studies the development of a laminar blood flow in a tube with a square and round cross-section under exposure to a magnetic field. The series of papers [35–38] also addressed the influence of a magnetic field on the current character in cavities.

Specifically, the authors of [35, 36] explore a fully developed laminar flow with the forced convection of electrically non-conducting viscous biomagnetic fluid in a cavity. The liquid is under the influence of a point magnetic source located under the cavity. In [37], authors study a three-dimensional flow of electricity conductive fluid in a cubic cavity with the movement of the upper wall and under the impact of the external magnetic field. It was found that the magnetic field significantly affects the circulation in the cavity and changes the shape and location of primary and secondary vortexes. As the magnetic field tension increases, the center of the main vortex shifts to the upper right corner.

The laminar magnetic natural convection in a square case filled with a porous medium is studied in [38] in order to investigate the effects of viscous dissipation and radiation. The medium that fills the case is heated from the left vertical side wall and cooled from the opposite right vertical side wall. The upper and lower walls of the case are considered adiabatic. The flow in the square case is exposed to a homogeneous magnetic field at different angles of orientation.

The author of work [39] reported a numerical simulation of the three-dimensional compressed flow around an open cavity. The work shows that the detected instability is hydrodynamic in character rather than acoustic, as it was assumed, and it arises due to the general instability of the current associated with the circulation of a vortex flow at the bottom of the cavity. The author notes an analogy of the established unstable circulations with similar phenomena when a step facing backwards is streamlined. The results obtained are consistent with the data from previous experiments, as well as with numerical studies into the flow around open cavities.

The series of papers [40, 41] consider basic approaches to modeling and acoustic patterns in the flow around cavities. Article [41] gives a detailed overview of the application and benefits of numerical algorithms for calculating parameters under a laminar current mode in cavities, as well as turbulent, based on RANS, LES, DES, DNS models. The effect of cavity geometry on the change in pressure field in its vicinity was investigated. Some active and passive methods for suppressing noise fluctuations in the cavity when it is streamlined were also considered.

An experimental study of the structure of the flow in a rectangular cavity is reported in work [42]. Measurements were performed using a wind tunnel with a low degree of flow turbulence. Based on measurements of static pressure values in the flow on the cavity wall, as well as sound pressure, the main parameters and features of vibrations in the flow in different types of resonators at low speed were studied. The influence of cavity geometry (the ratio of length to depth as well as width to depth) on the character of current in the cavity and noise characteristics was also determined.

Thus, as the above review demonstrates, among the many works published over recent years [6–42], which addressed current in pockets and cavities of different configurations, none has dealt with the task of studying the structure of a viscous flow in an open cavity considering the outer current in a channel above the cavity. The existence of a channel above the cavity leads to a complete rearrangement of the current pattern, it changes the distribution of velocities in the internal volume of the cavity, pressure and tangential stresses on its immobile walls compared to the current in a similar closed cavity without a channel.

Knowing the flow structure in a cavity makes it possible to apply methods to control the current, by changing the length and location of detachable zones in order to reduce the aerodynamic drag. A given task could find application in a variety of fields of science and technology, including: the flow around industrial buildings and structures, in rail-road transport – when the inter-car intervals of a moving high-speed train are flown around, at a bullet motion in a multi-chamber silencer, in the operation of a cannon barrel's ejector, when an open transition compartment connecting the stages of a rocket is flown around.

Reliable determination of the structure and parameters of the current in the internal volume of a cavity and in the boundary layer on its walls would make it possible to optimally control a flow in the cavity and reduce the resulting loads.

3. The aim and objectives of the study

The aim of this work is to numerically determine the structure of a circulating detachable laminar flow of the

viscous incompressible liquid in an open cavity taking into consideration the outer current. Features in the current structure determine the distribution of pressure and tangential stresses on the stationary walls of the cavity.

To accomplish the aim, the following tasks have been set:

- to numerically integrate the Navier-Stokes system of differential equations under a laminar current mode by employing the numerical method of finite elements as a tool;

- to verify the devised procedure using a test problem about the flow of a viscous incompressible liquid in a cubic cavity with a movable face;

- to investigate, at the Reynolds' number value $Re=3,000$, the structure of vortex formation over the entire estimated area of the cavity current, as well as in the mixing layer and in the boundary layers on the walls of the cavity;

- to illustrate the resulting current by vorticity profiles, the thickness of the boundary layer, the constituents of speed components in different cross-sections of the cavity, in the boundary layers on the walls, as well as in the mixing layer;

- based on the results, to analyze the detachable current in the internal volume of the cavity.

4. Procedure for numerical study of a laminar detachable movement in an open cavity with the presence of a channel

The defining system of differential equations in the case of a laminar viscous incompressible current included the Navier-Stokes equations (2):

$$\frac{\partial u_i}{\partial t} + u_j \frac{\partial u_i}{\partial x_j} = F_i - \frac{1}{\rho} \frac{\partial p}{\partial x_i} + \nu \nabla^2 u_i,$$

$$i, j = \overline{1, 3}, \tag{2}$$

as well as continuity equation (3)

$$\frac{\partial u_j}{\partial x_j} = 0, \quad j = \overline{1, 3}. \tag{3}$$

The procedure for applying the numerical method of finite elements to the integration of a system of differential equation is given in [6].

5. Results of studying the structure of a detachable movement in an open cavity with the presence of a channel

The built calculation algorithm was tested on the problem about a flowing viscous incompressible liquid in a cubic cavity with a movable face. The results obtained were compared with the results reported in [43]. The comparison was based on the following magnitudes: patterns of current functions, the profiles of the longitudinal and transverse components of speed in the central cross-sections of the cavity, the fields of isolines of speed components. Also compared were the isobars of static and full pressure, the horizontal and vertical profiles of pressure factor in the cross-section along the center of the vortex, the distribution of pressure factor and

tangential stresses along the walls of the cavity, the trajectories of liquid particles introduced to the cavity in its various regions. Results from some of the author's calculations are reported in [8]. Satisfactory alignment of estimated data has made it possible to proceed to studying the problem on a current in the open cavity.

Fig. 1–4 show profiles of the longitudinal and transverse speed components, as well as vorticity in different cross-sections of the cavity at $Re=3,000$; in addition, Fig. 1–4 include experimental data [44]. The different color of symbols corresponds to different cross-sections of the cavity.

The magnitude $Re=3,000$ was calculated by analogy to data from [44] and corresponded to the laminar current of the assigned input profile in a channel above the cavity.

The shape of curves in the graphs from Fig. 1–4 shows that the overall current in the inner volume of the cavity and in the channel above it can be divided into several large regions. The central vortex forms the main circulation movement in the cavity. The secondary circulation motion in the cavity is composed of smaller secondary vortices located in the lower corners of the cavity. The region adjacent to the upper cut of the cavity, which forms following the flow detachment in the upper left corner of the cavity, is a mixing zone.

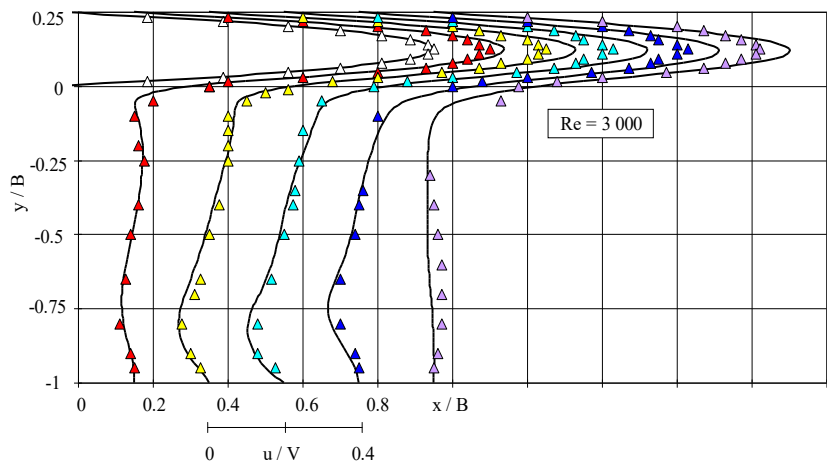


Fig. 1. Profiles of velocity components $u_x=U$ in different cross-sections of the cavity at $Re=3,000$ compared to data from [44]

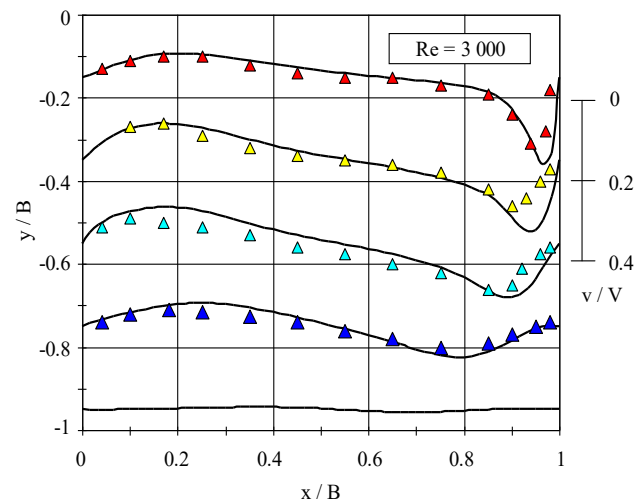


Fig. 2. Profiles of velocity components $u_y=V$ in different cross-sections of the cavity at $Re=3,000$ compared to data from [44]

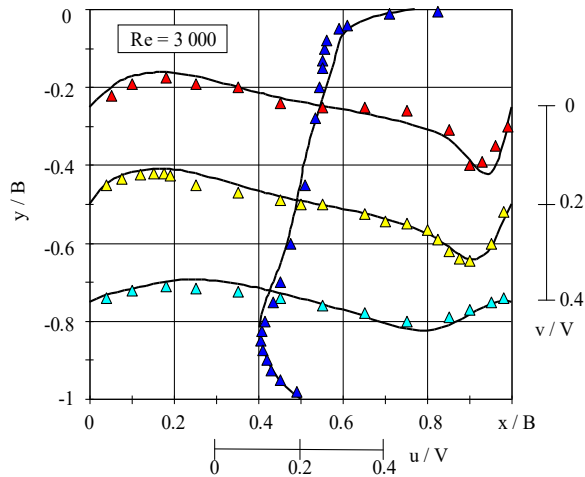


Fig. 3. Profiles of velocity components: component U (cross-section $X=0.5$) and component V (cross-sections $Y=0.25; 0.5; 0.75$) at $Re=3,000$, Δ – [44, 45]

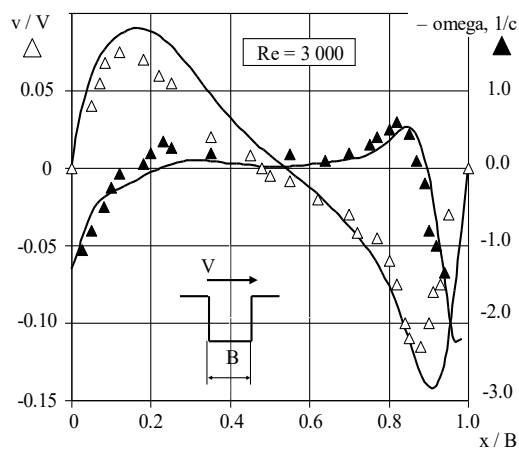


Fig. 4. Distribution, at $Re=3,000$, of the transverse component of speed and vorticity in a plane parallel to the bottom of the cavity and located at a distance from it equal to half its height, Δ , \blacktriangle – [44]

Downstream, the mixing zone is expanding; reaching the right vertical wall, a stream of liquid from the mixing zone spreads across all the walls of the cavity, forming a near-wall boundary layer. Fig. 1, 2 show the velocity profiles in the following cross-sections: the longitudinal (transverse) speed component: $X(Y)=0.15; 0.35; 0.55; 0.75; 0.9$. Verification of the results obtained against data from [44] shows that in certain zones of the examined region there is some discrepancy between the estimated speed profiles and experimental data. Specifically, there is a mismatch between values of longitudinal speed component X along the axis of the channel over the cavity: the estimated curves indicate a more intense movement of the fluid in the central part of the channel than it was recorded in the experiment, and the degree of divergence increases downwards the flow. There is also a discrepancy between the values of the transverse constituent of speed component near the right-hand vertical wall. In contrast to experimental data, the estimated curves indicate a much smaller thickness of the boundary layer near this wall. A given disagreement can be probably explained by the purely technical inability to acquire high quality measurements near a rigid wall during the experiment.

It should be noted that in determining a Reynolds number, the authors of work [44] used the width of the channel as a characteristic linear size, so the Reynolds number specified in the cited work is much smaller than the Reynolds number calculated for the width of the cavity, as is the case for the current study and in most authors of other works.

Analysis of the alignment of estimated speed profiles with experimental data from [45], shown in Fig. 3, reveals a more satisfactory coincidence, compared to Fig. 1, 2, of the transverse velocity component in the central horizontal cross-section near a right-hand vertical wall. This fact, apparently, can be explained by the exclusion of the impact exerted by side effects on the structure of a fluid circulation motion in the cavity embedded in the experimental setup.

Curves in Fig. 4 represent: the profile of a transverse velocity component in the central horizontal cross-section of the cavity, as well as a change in vorticity in the same cross-section in comparison with data from [44]. The vorticity was calculated from the following formula

$$\omega = \frac{1}{2} \left[\frac{\partial v}{\partial x} - \frac{\partial u}{\partial y} \right]. \tag{4}$$

Analysis of Fig. 4 confirms the existence, in the center of the cavity, of a vortex, characterized by the constant vorticity. In the region of a boundary layer near the walls, vorticity changes the sign to the opposite.

The mixing zone. Fig. 5 shows the profiles of a longitudinal constituent of the speed component in the mixing region for the following cavity cross-sections: $X=0.25; 0.35; 0.55; 0.65; 0.75; 0.95$. For comparison, experimental data from [44] are drawn in the respective cross-sections (triangles) and a Hagen-Poiseuille velocity profile [3], assigned in the channel's inlet cross-section over the cavity (circles) as follows

$$\frac{u}{u_0} = 4 \left(\frac{y}{h} \right) - 4 \left(\frac{y}{h} \right)^2, \tag{5}$$

where h is the width of a channel.

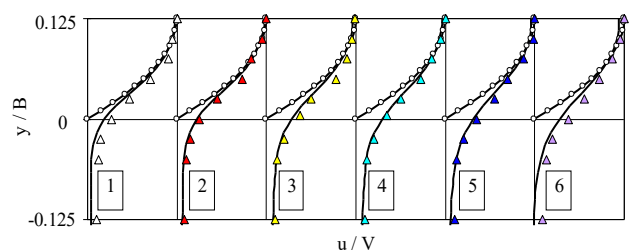


Fig. 5. Profiles of the longitudinal constituent of a speed component in the mixing zone for several cross-sections at $Re=3,000$: $x/B=0.25$ – curve 1; 0.35 – curve 2; 0.55 – curve 3; 0.65 – curve 4; 0.75 – curve 5; 0.95 – curve 6; – [44]

The figure shows an almost complete match between speed profiles in all cross-sections of the jet, and, in the region adjacent to the $y/B=0.125$ line, which is the axis of the channel, a match between the estimated profiles and the Hagen-Poiseuille profile.

The boundary layer. Fig. 6, 7 show, respectively, the speed profile at the outer border of the boundary layer and a change in its thickness on the stationary walls of the cavity, as well as the shape parameter Λ distribution curve along

the longitudinal coordinate. Fig. 6 characterizes a change in speed on the outer border of the boundary layer (curve 1) and the magnitude of thickness of the boundary layer on the stationary walls of the cavity (curve 2). The outer border of the boundary layer was determined, similarly to [44], based on the maximum value of the return current speed near the wall. The ordinate axis of the graph carries relative magnitudes of the corresponding components of speed (the longitudinal component at the bottom and the transverse one on the two vertical walls of the cavity), the abscissas axis depicts the stationary walls of the cavity conditionally deployed on the plane.

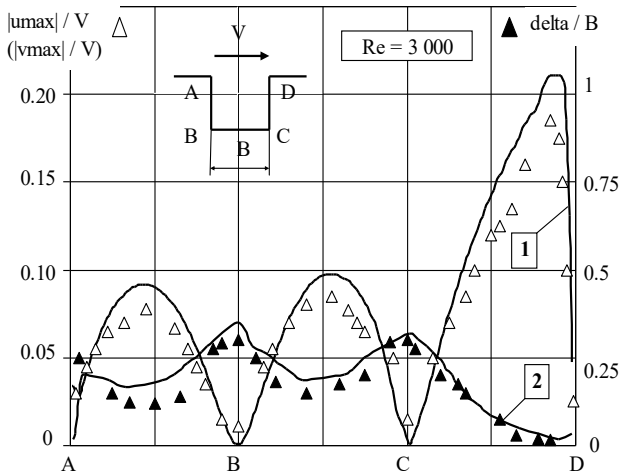


Fig. 6. Distribution of speed on the outer border of the boundary layer and of values for the thickness of the boundary layer on the stationary walls of the cavity at Re=3,000, Δ , \blacktriangle – [44]

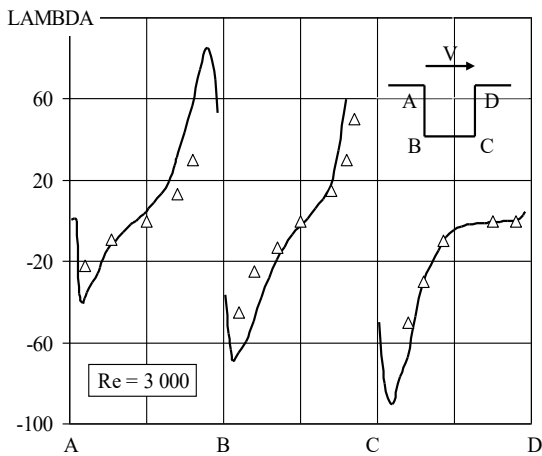


Fig. 7. Distribution of shape parameter Λ along the longitudinal coordinate at Re=3,000, Δ – [44]

The character of curve change in Fig. 6 shows that the values of relative magnitudes of velocity in the middle parts of the front (AB) wall and the bottom (BC) of the cavity are almost identical. At the same time, curve 1 reaches its maximum near the angular point D, in the vicinity of which there is a mixing of liquid from the internal volume of the cavity with a powerful external jet of the mixing zone.

The minima of curve 1 are observed at the angular points B and C, where the relative velocity drops to zero.

The reverse character of change is demonstrated by curve 2, which characterizes values for the thickness of

the boundary layer on the stationary walls of the cavity. A maximum is reached by curve 2 at the points of a minimum of curve 1 – at the angular points B and C, which is predetermined by the existence of secondary components of circulation. In the central parts of the walls AB and BC the thicknesses of the boundary layer coincide and decrease in magnitude in comparison with the corresponding thickness magnitudes in the lower corners of the cavity. A minimum is reached by curve 2 at point D, which is due to the almost complete destruction of the boundary layer in this region when in collision with the external stream of the channel.

By knowing the change in characteristics of the boundary layer, shown in Fig. 6, it is possible to build the shape parameter distribution along the length of the stationary walls of the cavity, shown in Fig. 7. The shape parameter was calculated from the following formula

$$\Lambda = \frac{\delta^2}{\nu} \cdot \frac{du_{max}}{dx}, \quad (6)$$

that made it possible to determine the effect of the longitudinal speed gradient on the characteristics of the laminar boundary layer. The procedure for building Fig. 7 is identical compared to Fig. 6: the ordinate axis maps the examined magnitude – a shape parameter, the abscissa axis is formed by the stationary walls of the cavity deployed along a horizontal straight line.

Comparing the resulting shape parameter curves with the experimental data from work [44] testifies to satisfactory agreement between the results in the central parts of the stationary walls. Discrepancies in the magnitudes of the shape parameter were observed only in the vicinity of cavity's corner points A, B and C, where, in contrast to experimental points, the estimated curves have local extrema.

Fig. 8 shows, in the cavity's several cross-sections, the profiles of the transverse constituent of a velocity component for the thickness of the boundary layer on the left (Fig. 8, a) and the right (Fig. 8, b) walls of the cavity. Fig. 9 illustrates the profiles of the longitudinal constituent of a velocity component for the thickness of the boundary layer at the bottom (Fig. 9) of the cavity under a laminar fluid movement mode.

The graphs are built in dimensionless coordinates, assigned to the corresponding characteristics of the boundary layer: the values for speed components are assigned to the speed at the outer border of the boundary layer, the linear size – to the thickness of the boundary layer. When building Fig. 8, 9, the border of the boundary layer was determined based on the coordinates of the point near the wall, at which the speed of return movement reached a maximum. The curves carry experimental data from papers [44, 46, 47], as well as the theoretical profile by Polhausen for a flat boundary layer formed on the plate [48].

$$\frac{u}{u_m} = 2 \cdot \frac{y}{\delta} - 2 \cdot \left(\frac{y}{\delta}\right)^3 + \left(\frac{y}{\delta}\right)^4 + \frac{1}{6} \cdot \Lambda \cdot \frac{y}{\delta} \cdot \left(1 - \frac{y}{\delta}\right)^3, \quad (7)$$

where Λ is the shape parameter derived from formula (6).

The Polhausen profile is mapped not for all speed profiles, but only to those that show a satisfactory match between values. Such profiles are located in the middle parts of the cavity walls, which confirms the hypothesis about inapplicability of the Polhausen profile in the diffuser zone,

expressed in the expansion of the flow and a decrease in speed, which exists in the corners of the cavity due to the secondary vortexes circulating in these regions.

Fig. 8, 9 show that near the lower corners of the cavity the circulation of secondary vortexes leads to the reformation of the velocity profile for the thickness of the boundary layer. In this case, the current in the boundary layer changes from such that is filled over most of the fixed walls to the detachable one in the vicinity of the lower corners of the cavity. This is qualitatively consistent with the results from the Polhausen's calculation for a flat boundary layer taking into consideration the pressure gradient.

This proves the fact that the boundary layer, which develops on the walls of the cavity, is qualitatively different from a regular boundary layer on the plate when it is laminarly flown around; it is impossible to apply the same methods for its calculation.

Thus, the numerical study of the laminar flow of a viscous incompressible liquid in an open cavity, taking into consideration the external flow in a channel above the cavity, has made it possible to determine the structure of the circulation movement in it:

1) the central part of the cavity is occupied by the main vortex, which has a constant vorticity;

2) the secondary current in the cavity is less long compared to the central vortex of secondary vortexes located in the lower corners of the cavity;

3) the mixing zone occupies the upper region of the cavity and is formed after the flow detaches from the left horizontal wall of the channel over the cavity,

4) the length of the mixing zone increases when approaching the right vertical wall of the cavity and it forms a boundary layer first on the specified wall, and then on all other rigid walls of the cavity;

5) a boundary layer on the walls of the cavity is formed when the liquid flows around from the mixing zone, it is characterized by an opposite sign change in vorticity compared to the main circulation current.

Analysis of the structure and character of fluid movement in a cavity with a channel has made it possible to establish the following patterns:

1) the greatest degree of fluid mixing in the cavity is noted in two regions. A first region is the vicinity of the right corner point of the cavity, where the developed current from the mixing zone interacts with the main current of the cavity. A second region is characterized by the movement of fluid from the boundary layer near the right vertical wall of the cavity, which leads to the almost complete destruction of the boundary layer near the right upper corner of the cavity;

2) the least degree of mixing is implemented in the regions of current with the maximum thickness of the boundary layer – in the lower corners of the cavity, characterized by the developed secondary current, represented by angular circulation vortexes.

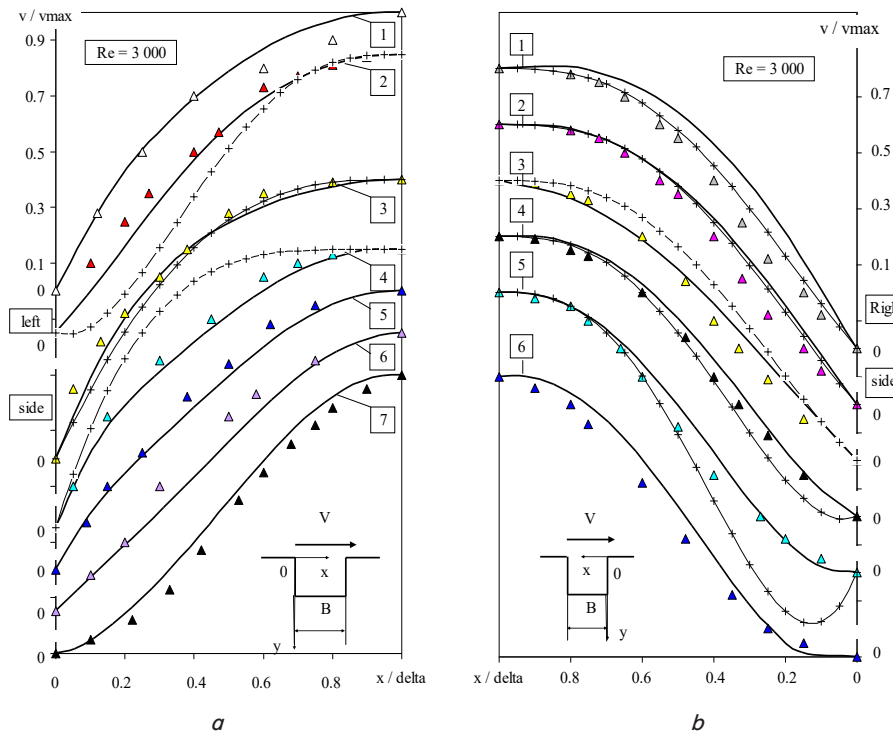


Fig. 8. Velocity profiles for the thickness of the boundary layer on the cavity's vertical walls at $Re=3,000$: *a* – left wall: $y/B=0.10$ – curve 1; 0.25 – curve 2; 0.50 – curve 3; 0.70 – curve 4; 0.75 – curve 5; 0.80 – curve 6; 0.85 – curve 7; *b* – right wall: $y/B=0.35$ – curve 1; 0.45 – curve 2; 0.50 – curve 3; 0.60 – curve 4; 0.70 – curve 5; 0.75 – curve 6; Δ – [43], $-+-$ [46, 47]

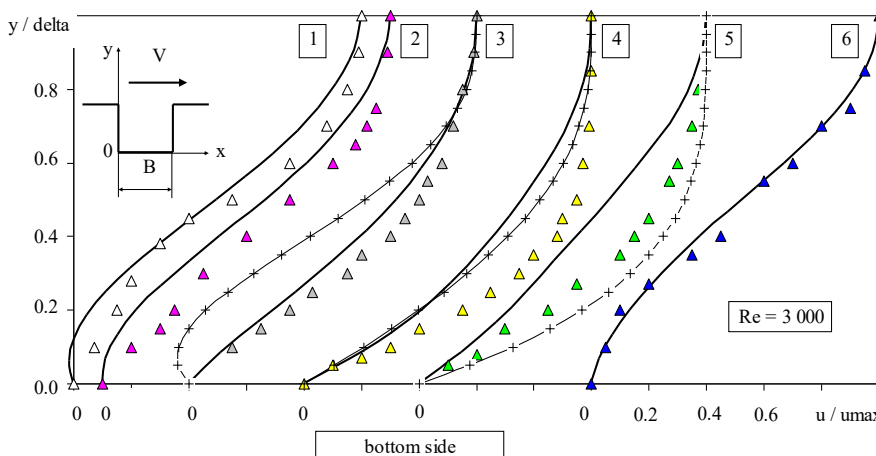


Fig. 9. Profiles of the longitudinal velocity component for the thickness of the boundary layer at the cavity's bottom at $Re=3,000$: $x/B=0.15$ – curve 1; 0.20 – curve 2; 0.35 – curve 3; 0.55 – curve 4; 0.65 – curve 5; 0.75 – curve 6; Δ – [43], $-+-$ [46, 47]

6. Discussion of results from studying a detachable laminar current in an open cavity taking into consideration the external flow in the channel

In order to integrate the system of Navier Stokes equations, an algorithm based on a finite element method was constructed; it was verified using a test problem about the flow of a viscous incompressible liquid in a cubic cavity with a movable face. Difference between own estimated data and those found in the scientific literature did not exceed 5 % for numerical solutions and 15 % for experimental works, which can be explained by features in numerical modeling as an approximate technique, as well as by the human factor and errors in the equipment during experimental studies.

The structure of vortex formation in an open cavity has been investigated, as well as in the mixing layer and in the boundary layers on its walls, at Reynolds number $Re=3,000$. The resulting current was illustrated by the profiles of vorticity, the thickness of the boundary layer, the constituents of speed components in the various cross-sections of the cavity, in the boundary layers on the walls, as well as in the mixing layer. An analysis of detachable current in the internal volume of a cavity has been performed, given in the main text of this paper.

The benefits of solutions obtained are due to the versatility of a finite element method as a numerical method, as well as to the detailed treatment of calculation parameters resulting from numerical modeling.

Within the framework of the study described in the current work, the structure of the main and secondary circulation currents in an open cavity, taking into consideration the outer current in a channel above it, has been determined. This eliminates the rectilinear character of a current line connecting the upper corners of the cavity – the drawback in the statement of a problem about liquid motion in a closed cavity with a movable wall. Another advantage of this study worth considering is the procedure – application of the numerical method of finite elements, which makes it possible to study in detail the structure of a flow in the boundary layers directly on the walls of the cavity, which is difficult technologically when performing field experiments.

The established flow structure and a vortex formation system make it possible to control jet currents inside the internal volume of a cavity, and, consequently, to optimize the aerodynamic forces acting on the cavity. Specifically, it is possible to reduce the aerodynamic drag of the cavity, which acts on its rigid walls when they are flown around. The applied aspect in implementing the obtained scientific result is the possibility to use it to the flow around industrial objects: buildings, inter-car intervals in a railroad train, etc.

The research in this field is continuation of previous numerical experiments involving numerical study into the hydrodynamics of detachable flat and spatial currents when the industrial facilities and their elements are streamlined.

The resulting numerical solution, visualized with the help of constructed graphs, makes it possible to establish with the necessary degree of accuracy the structure of a viscous laminar detachable current in an open cavity with the presence of an external current above it, as well as to detail vortex flows into the main, secondary vortex regions, a mixing zone, and a current in the boundary layer. The reliability of results obtained has been confirmed by verification and can be explained by a rather small error of the numerical

method, which, in turn, is achieved by a detailed computational grid at numerical modeling.

When applying the results obtained here to practical tasks, it is necessary to take into consideration the two-dimensional statement of the set problem. This means that its consideration implies an open cavity, for which its length in the direction perpendicular to the plane of the current far exceeds the width/height of the wall.

The disadvantages of the current study worth noting are the lack of a study into the effect exerted on the structure of current by different speeds of the outer flow in a channel over the cavity and the lack of influence exerted on the structure of current by the ratio “width/height” of the cavity.

The methodology of this study can also be extended to solve three-dimensional problems about detachable currents in cavities of different configurations.

7. Conclusions

1. A numerical integration of the system of Navier Stokes differential motion equations under a laminar current mode has been performed using a finite element method: a calculation algorithm has been built.

2. The built algorithm was verified by solving a test problem about the laminar motion of a viscous incompressible fluid in a cubic cavity with a movable face, with the result confirming the reliability of the algorithm used. Comparison between the following estimated data and known results reported by other authors was performed: patterns in current functions, profiles of the longitudinal and transverse components of speed in the central cross-sections of the cavity, fields of isolines of speed components. Also compared were the isobars of static and full pressures, the horizontal and vertical profiles of pressure factor in the cross-section along the center of the vortex, the distribution of pressure factor and tangential stresses along the walls of the cavity, the trajectories of liquid particles introduced to the cavity in its various regions.

3. A numerical calculation of the laminar viscous current at $Re=3,000$ in the open cavity has been carried out, taking into consideration the external flow in a channel above the cavity. The calculation results acquired were visualized by patterns in current, velocity and vorticity profiles, the thickness of the boundary layer in the entire estimated current region of the cavity, as well as in the mixing layer and in the boundary layers on the walls of the cavity. The resulting graphic information has made it possible to analyze the flow structure in an open cavity and to represent in detail the patterns in its development.

4. An analysis of the flow structure has revealed the existence, length, and location of vortex streams in an open cavity with the presence of a channel above it.

5. Based on the analysis of the laminar viscous current in an open cavity with a channel, the structure of the current in it has been determined, the regions with the main and secondary circulation movement have been defined, as well as the boundary layer and the mixing zones. The main vortex movement in an open cavity is formed by a central vortex, occupying the bulk of the cavity, and located in the region of its geometric center. The secondary vortex movement is formed by circulations of less intensity, compared to the central vortex, and located in the lower corners of the cavity. The mixing zone is formed as a result of flow detachment

from the left vertical wall of the cavity and expands when approaching the right vertical wall. The current in a boundary layer is opposite to the main current in the cavity.

Acknowledgement

This paper is dedicated to the memory of the Teacher Professor, Doctor of Physics and Mathematics, Mr. Alexander Alexeyevich Kochubey. He was a specialist in the field of numerical modeling of hydrodynamics and heat-exchange processes in complex geometry systems based on a finite element method. He was among the first in Ukraine to start the development and application, using finite elements, of new approximation functions, based on particular solutions to the model equations of substance transfer. He is

the author of more than 120 scientific works, including two monographs, seven training-teaching aids. He was a member of the National Committee of Ukraine on Theoretical and Applied Mechanics, Vice-Chairman of two specialized councils for defending candidate and doctoral theses, he led a series of research papers on the scientific activities at the Dnipro Oles Honchar National University. He was elected a member of the Academy of Education Information Sciences (Russia), a member of the Interregional Academy of Social Technologies and Local Government (Russia), and a member of the Ukrainian Environmental Academy of Sciences. He was awarded the Honorary Letter from the Ministry of Education and Science in Ukraine, the Honorary Letter from the Parliament of Ukraine, and was awarded the title "Excellence in education of Ukraine" (2002) as well as the honorary title "Honored Scientist of Ukraine" (2002).

References

1. Chzhen, P. (1972). *Otryvnye techeniya*. Vol. 1. Moscow: Mir, 299.
2. Krasnov, N. F., Koshevoy, V. N., Kalugin, V. P. (1988). *Aerodinamika otryvnykh techeniy*. Moscow: Vysshaya shkola, 351.
3. Shlihting, G. (1969). *Teoriya pogranichnogo sloya*. Moscow: Nauka, 744.
4. Simuni, L. M. (1965). Chislennoe reshenie zadachi dvizheniya zhidkosti v pryamougol'noy yame. *PMTE*, 6, 106–108.
5. Charwat, A. F., Dewey, C. F., Roos, J. N., Hitz, J. A. (1961). An Investigation of Separated Flows- Part I I: Flow in the Cavity and Heat Transfer. *Journal of the Aerospace Sciences*, 28 (7), 513–527. doi: <https://doi.org/10.2514/8.9099>
6. Kravets, E. V. (2005). Matematicheskoe modelirovanie turbulentnykh techeniy vyzkoy neszchimaemoy sredy v mezhvagonnom prostranstve s kryshnym obtekatelom. *Visnyk DNU. Seriya: Mekhanika*, 1 (10), 66–73.
7. Kochubey, A. A., Kravets, E. V. (2012). Sravnitel'nyy analiz chislennykh i analiticheskikh issledovaniy tsirkulyatsionnykh dvumernykh techeniy v kavernah. *Tekhnicheskaya mehanika*, 1, 38–55.
8. Kochubey, A. A., Kravets, E. V. (2013). Analiz eksperimental'nykh i chislennykh issledovaniy vkhvnykh techeniy v trekhmernykh kavernah. *Visnyk Dnipropetrovskoho universytetu. Seriya: Mekhanika*, 21 (17 (1)), 51–63.
9. Terehov, V. I., Kalinina, S. V. (2002). Struktura techeniya i teploobmen pri obtekanii edinichnoy sfericheskoy kaverny. Sostoyanie voprosa i problemy (obzor). *Teplofizika i aeromehanika*, 4, 497–520.
10. Terekhov, V. I., Kalinina, S. V., Mshvidobadze, Yu. M. (1994). Heat transfer from a spherical cavity located on a rectangular channel wall. *Teplofizika vysokikh temperatur*, 32 (2), 249–254.
11. Mironov, D. S. (2011). Eksperimental'noe issledovanie pul'satsiy davleniya, generiruemym melkoy otkrytoy kavernoy, s primeneniem chastotno-vremennykh metodov obrabotki dannykh. *Teplofizika i aeromehanika*, 18 (3), 385–395.
12. Terekhov, V. I., Kalinina, S. V., Sharov, K. A. (2012). Features of flow and heat transfer for the jet interaction with a spherical cavity-shaped obstacle with a round edge. *High Temperature*, 50 (2), 295–297. doi: <https://doi.org/10.1134/s0018151x12020198>
13. Burtsev, S., Vinogradov, Y., Kiselev, N., Strongin, M. (2016). Selection of Rational Heat Transfer Intensifiers in the Heat Exchanger. *Science and Education of the Bauman MSTU*, 12, 35–56. doi: <https://doi.org/10.7463/1216.0852444>
14. Pavan Kumar Reddy, M., Ramana Murthy, J. V. (2019). Entropy analysis for heat transfer in a rectangular channel with suction. *Heat Transfer-Asian Research*, 48 (7), 2773–2798. doi: <https://doi.org/10.1002/htj.21513>
15. Biswas, N., Manna, N. K. (2017). Transport phenomena in a sidewall-moving bottom-heated cavity using heatlines. *Sādhanā*, 42 (2), 193–211. doi: <https://doi.org/10.1007/s12046-016-0586-4>
16. Curi, M., De Sampaio, P. A. B., Gonçalves Junior, M. A. (2017). Study of natural convection with a stabilized finite element formulation. *Computational Thermal Sciences: An International Journal*, 9 (6), 513–527. doi: <https://doi.org/10.1615/computthermalsci.2017018186>
17. Purusothaman, A., Baïri, A., Nithyadevi, N. (2016). 3D natural convection on a horizontal and vertical thermally active plate in a closed cubical cavity. *International Journal of Numerical Methods for Heat & Fluid Flow*, 26 (8), 2528–2542. doi: <https://doi.org/10.1108/hff-08-2015-0341>
18. Roy, M., Basak, T., Roy, S. (2015). Analysis of Entropy Generation During Mixed Convection in Porous Square Cavities: Effect of Thermal Boundary Conditions. *Numerical Heat Transfer, Part A: Applications*, 68 (9), 925–957. doi: <https://doi.org/10.1080/10407782.2015.1023134>
19. Umavathi, J. C., Ojjela, O., Vajravelu, K. (2017). Numerical analysis of natural convective flow and heat transfer of nanofluids in a vertical rectangular duct using Darcy-Forchheimer-Brinkman model. *International Journal of Thermal Sciences*, 111, 511–524. doi: <https://doi.org/10.1016/j.ijthermalsci.2016.10.002>
20. Ternik, P., Buchmeister, J. (2015). Buoyancy-Induced Flow and Heat Transfer of Power Law Fluids in a Side Heated Square Cavity. *International Journal of Simulation Modelling*, 14 (2), 238–249. doi: [https://doi.org/10.2507/ijimm14\(2\)5.293](https://doi.org/10.2507/ijimm14(2)5.293)

21. Rashad, A., Mansour, M., Gorla, R. S. R. (2016). Mixed convection from a discrete heater in lid-driven enclosures filled with non-Newtonian nanofluids. *Proceedings of the Institution of Mechanical Engineers, Part N: Journal of Nanomaterials, Nanoengineering and Nanosystems*, 231 (1), 3–16. doi: <https://doi.org/10.1177/1740349916634749>
22. Polyakov, A. F. (2014). A steady viscous-thermogravitational flow of capillary liquid and heat transfer in a vertical cavity under asymmetric heat conditions. *High Temperature*, 52 (1), 72–77. doi: <https://doi.org/10.1134/s0018151x14010179>
23. Aksouh, A., Mataoui, A., Seghouani, N. (2012). Low Reynolds-number effect on the turbulent natural convection in an enclosed 3D tall cavity. *Progress in Computational Fluid Dynamics, An International Journal*, 12 (6), 389. doi: <https://doi.org/10.1504/pcfd.2012.049811>
24. Noori Rahim Abadi, S. M. A., Jafari, A. (2012). Investigating the natural convection heat transfer from two elliptic cylinders in a closed cavity at different cylinder spacings. *Heat Transfer Research*, 43 (3), 259–284. doi: <https://doi.org/10.1615/heattransres.2012002036>
25. Kaluri, R. S., Basak, T. (2011). Role of entropy generation on thermal management during natural convection in porous square cavities with distributed heat sources. *Chemical Engineering Science*, 66 (10), 2124–2140. doi: <https://doi.org/10.1016/j.ces.2011.02.009>
26. Bouabid, M., Magherbi, M., Hidouri, N., Brahim, A. B. (2011). Entropy Generation at Natural Convection in an Inclined Rectangular Cavity. *Entropy*, 13 (5), 1020–1033. doi: <https://doi.org/10.3390/e13051020>
27. Boger, A. A., Ryabov, S. V., Ryazhskikh, V. I., Slyusarev, M. I. (2010). Calculation of a conductive-laminar thermo-convection regime of a Newtonian fluid in a rectangular cavity with isothermal vertical boundaries. *Fluid Dynamics*, 45 (3), 355–358. doi: <https://doi.org/10.1134/s0015462810030026>
28. Bulat, A., Blyuss, B., Dreus, A., Liu, B., Dziuba, S. (2019). Modelling of deep wells thermal modes. *Mining of Mineral Deposits*, 13 (1), 58–65. doi: <https://doi.org/10.33271/mining13.01.058>
29. Asadi, H., Javaherdeh, K., Ramezani, S. (2013). Finite element simulation of micropolar fluid flow in the lid-driven square cavity. *International Journal of Applied Mechanics*, 05 (04), 1350045. doi: <https://doi.org/10.1142/s1758825113500452>
30. Yamouni, S., Mettot, C., Sipp, D., Jacquin, L. (2013). Passive Control of Cavity Flows. *Journal AerospaceLab*, 6, 1–7.
31. Nagarajan, K. K., Singha, S., Cordier, L., Airiau, C. (2018). Open-loop control of cavity noise using Proper Orthogonal Decomposition reduced-order model. *Computers & Fluids*, 160, 1–13. doi: <https://doi.org/10.1016/j.compfluid.2017.10.019>
32. Iorio, C. S., Goncharova, O., Kabov, O. (2011). Influence of Boundaries on Shear-driven Flow of Liquids in Open Cavities. *Microgravity Science and Technology*, 23 (4), 373–379. doi: <https://doi.org/10.1007/s12217-011-9257-6>
33. González, L. M., Ahmed, M., Kühnen, J., Kuhlmann, H. C., Theofilis, V. (2011). Three-dimensional flow instability in a lid-driven isosceles triangular cavity. *Journal of Fluid Mechanics*, 675, 369–396. doi: <https://doi.org/10.1017/s002211201100022x>
34. Senel, P., Tezer-Sezgin, M. (2018). Convective Flow of Blood in Square and Circular Cavities. *Analele Universitatii "Ovidius" Constanta - Seria Matematica*, 26 (2), 209–230. doi: <https://doi.org/10.2478/auom-2018-0026>
35. Senel, P., Tezer-Sezgin, M. (2016). DRBEM solution of biomagnetic fluid flow and heat transfer in cavities-CMMSE2016. *Journal of Mathematical Chemistry*, 55 (7), 1407–1426. doi: <https://doi.org/10.1007/s10910-016-0721-9>
36. Senel, P., Tezer-Sezgin, M. (2016). DRBEM solutions of Stokes and Navier–Stokes equations in cavities under point source magnetic field. *Engineering Analysis with Boundary Elements*, 64, 158–175. doi: <https://doi.org/10.1016/j.enganabound.2015.12.007>
37. Jin, K., Vanka, S. P., Thomas, B. G. (2015). Three-Dimensional Flow in a Driven Cavity Subjected to an External Magnetic Field. *Journal of Fluids Engineering*, 137 (7). doi: <https://doi.org/10.1115/1.4029731>
38. Ahmed, S. E., Hussein, A. K., Mohammed, H. A., Adegun, I. K., Zhang, X., Kolsi, L. et. al. (2014). Viscous dissipation and radiation effects on MHD natural convection in a square enclosure filled with a porous medium. *Nuclear Engineering and Design*, 266, 34–42. doi: <https://doi.org/10.1016/j.nucengdes.2013.10.016>
39. Br s, G. A., Colonius, T. (2008). Three-dimensional instabilities in compressible flow over open cavities. *Journal of Fluid Mechanics*, 599, 309–339. doi: <https://doi.org/10.1017/s0022112007009925>
40. Sinha, J. (2013). Studies on the Transition of the Flow Oscillations over an Axisymmetric Open Cavity Model. *Advanced in Aerospace Science and Applications*, 3 (2), 83–90.
41. Sinha, J., Arora, K. (2017). Review of the flow-field analysis over cavities. 2017 International Conference on Infocom Technologies and Unmanned Systems (Trends and Future Directions) (ICTUS). doi: <https://doi.org/10.1109/ictus.2017.8286128>
42. Yang, G., Sun, J., Liang, Y., Chen, Y. (2014). Effect of Geometry Parameters on Low-speed Cavity Flow by Wind Tunnel Experiment. *AASRI Procedia*, 9, 44–50. doi: <https://doi.org/10.1016/j.aasri.2014.09.009>
43. Isaev, S. A., Sudakov, A. G., Luchko, N. N., Sidorovich, T. V., Harchenko, V. B. (2002). Chislennoe modelirovanie laminarnogo tsirkulyatsionnogo techeniya v kubicheskoy kaverne s podvizhnoy gran'yu. *Inzhenerno-fizicheskiy zhurnal*, 75 (1), 49–53.
44. Bogatyrev, V. Ya., Dubnischchev, Yu. N., Muhin, V. A., Nakoryakov, V. E., Sobolev, V. S., Utkin, E. N., SHmoylov, N. F. (1976). Eksperimental'noe issledovanie techeniya v transhee. *PMTE*, 2, 76–86.
45. Bogatyrev, V. Ya., Gorin, A. V. (1976). O tortseyvyh effektakh v transheyah pryamougol'nogo poperechnogo secheniya. *Gradientnye i otryvnye techeniya*. Novosibirsk, 132–139.
46. Kármán, T. V. (1921). Über laminare und turbulente Reibung. *ZAMM - Journal of Applied Mathematics and Mechanics / Zeitschrift Für Angewandte Mathematik Und Mechanik*, 1 (4), 233–252. doi: <https://doi.org/10.1002/zamm.19210010401>
47. Pohlhausen, K. (1921). Zur näherungsweise Integration der Differentialgleichung der Iaminaren Grenzschicht. *ZAMM - Journal of Applied Mathematics and Mechanics. Zeitschrift Für Angewandte Mathematik Und Mechanik*, 1 (4), 252–290. doi: <https://doi.org/10.1002/zamm.19210010402>
48. Loytsyanskiy, L. G. (1970). *Mehanika zhidkosti i gaza*. Moscow: Nauka, 904.